Postprint version of of the paper published in J Nanopart Res 19, 196 (2017). https://doi.org/10.1007/s11051-017-3870-2

One-step synthesis, toxicity assessment and degradation in tumoral pH environment of SiO_2@Ag core/shell nanoparticles

Valeria De Matteis*[1], Loris Rizzello[2], Maria Pia Di Bello[3], Rosaria Rinaldi[1]

1. Università del Salento, Dipartimento di Matematica e Fisica "Ennio De Giorgi", Via Arnesano, 73100 Lecce, Italy
2. Department of Chemistry, University College London, London, WC1H 0AJ, UK
3. Università del Salento, Dipartimento di Ingegneria dell'Innovazione, Via Arnesano, 73100 Lecce, Italy

Corresponding Author: *e-mail: valeria.dematteis@unisalento.it

KEYWORDS: core/shell nanoparticles; one-step synthesis; cytotoxicity; genotoxicity; pH tumor environment; ionization

ABSTRACT

The unique physicochemical properties of SiO_2@Ag core/shell nanoparticles make them a promising tool in nanomedicine, where they are used as nanocarriers for several biomedical applications, including (but not restricted to) cancer treatment. However, a comprehensive estimation of their potential toxicity, as well as their degradation in the tumor microenvironment, has not been extensively addressed yet. We investigated *in vitro* the viability, the Reactive Oxygen Species (ROS) production, the DNA damage level, and the nanoparticles uptake on HeLa cells, used as model cancer cells. In addition, we studied the NPs degradation profile at pH 6.5, to mimic the tumor microenvironment, and at the neutral and physiological (pH 7- 7.4). Our experiments demonstrate that the silver shell dissolution is promoted under acidic conditions, which could be related to cell death induction. Our evidences demonstrate that SiO_2@Ag nanoparticles possess the ability of combining an effective cancer cells treatment (through local silver ions release) together with a possible controlled release of bioactive compounds encapsulated in the silica as future application.

INTRODUCTION

The extensive use on nanoparticles (NPs) in a plethora of research fields, such as diagnostic (Chen 2016), medical imaging (Rieffel 2015), and design of biomedical devices (Rodrigues 2016), has strengthened our knowledge of their physico-chemical properties, and all the possible ways to exploit them towards *ad hoc* applications. The NPs size, charge, shape, and surface characteristics all play a pivotal role in dictating the NPs behavior at the nanoscale (Nel 2009), especially while interacting with biological systems (Banerjeea 2016). Among all the NPs, core/shell NPs have been particularly investigated due to their unique and tunable properties (Wei 2011), as altering the metal shell around the inner core will lead to a completely new nano-object (Jackson 2001). These systems are often based on the use of silver, as this is known to combine a strong and sharp plasmon resonance band (Amendola 2010; Kneipp 1994), together with an enhanced toxicity in cancer cells (Nguyena 2016, Van der Zande 2016). We thus believed silver was the best candidate as a shell material in core/shell NPs. To this respect, there are already few works describing the toxicity of core/shell nanoparticles especially for cancer theranostics. In particular, the surfactants stabilizing the external metallic layer have been found to play a role in nanoparticles-driven toxicity (Fen 2013). In addition, experimental evidences reported that the cytotoxicity of AgNPs, coated with poly-(vinylpyrrolidone) (PVP), was due to their capacity to come in cells by endocytosis and localize into the lysosomes, an effect promoted by the PVP (Elbaz 2016). The degradation of nanoparticles in the lysosomes induces the release of silver ions, which are responsible of ROS production that are, in turns, the main cause of cell toxicity (Guo 2013, Zolghadri 2009). In addition, degradation phenomena could occur at typical pH that characterize microenvironment tumor cells. In fact the pH value tends to be more acidic (6.5) than healthy cells and blood (Ganta 2008): this important factor should be taken in consideration in the formulation of cancer therapy in order to understand the potential anticancer activity of these silver based nanomaterials. PVP-coated AgNPs have been proved to have anti-leukemia effect against multiple human AML cell lines and primary isolates from AML patients (Guo 2013). Additionally, AgNPs displayed anti-angiogenic effects through the inhibition of vascular endothelial

growth factor (VEGF) (Gurunathan 2013). A recent study underlined the hemo-compatibility of AgNPs on human erythrocytes that suggest their potential use as anticancer vector by intravenous administration (Huang 2016). An evolution of AgNPs, in terms of material design, is characterized by Ag-based core/shell NPs coated with PVP, which can combine the properties of two different materials in just one single vector. Hence, the scope of this work is to realize highly controlled NPs and to test their potential in cancer treatment. The fabrication of these nanostructures requires very low costing materials (SiO_2 and silver) and a short time of synthesis, as it is based on a "one-step synthesis". In general, there are many methods to deposit silver shells on silica surface, e.g. electroless plating techniques (Chang 2013), seed-mediated growth (Oldenburg 1998, Jiang 2003 Liu 2011, Choma 2011), silver deposition (Zsigmondy 1927), sonochemical processes (Pol 2002), thermal evaporation-based methods (Schueler 1993), via single electron transfer from octylamine to Ag^+ ions (Yang 2014) and multistep layer-by-layer deposition (Dong 2002, Cassagneau 2002). These techniques have the drawback of showing a poor level of surface coverage though, together with a lack of both uniform and/or monodispersed metallic coatings. Consequently, the metal NPs properties will display random and/or uncontrolled profiles, as they are strictly dependent on the NPs physicochemical characteristics (Westcott 2010, Dokoutchaev 1999). We developed here a highly customized and simple method for obtaining uniform silver shells on silica NPs. We did this by using of PVP as a stabilizing agent, in combination with different concentrations of silver nitrate. As reported above, the PVP choice regards not only your stabilization properties in the synthesis process but enhances the antitumor activities of nano-objects (Kanchana 2017). After a complete nanoparticles characterization, we evaluated their toxicity *in vitro* on epitheloid cervix carcinoma human cells line (HeLa) as model system. In particular, we investigated different effects on cells through several assays. WST-8 assay was used for evaluating cell viability, LDH assay to characterize cell membrane integrity, DCF assay for quantifying the ROS levels, and comet assay to check for DNA damage. We then moved the focus on understanding the toxicity mechanism, and we tested the effects upon NPs degradation (which leads to silver ions release) under acidic conditions. In particular, we tested the ionization of SiO_2@AgNPs at pH 6.5 that is a common value characterizing the microenvironment around tumor cells.

Experimental section

Materials

Silver Nitrate ($AgNO_3$), Poly-(vinylpyrrolidone) (PVP, MW ~55000), Tin(II) chloride ($SnCl_2$), Acetone, Tetraethyl Orthosilicate (TEOS, reagent grade, 98%), Ethanol (98%), Butanol, Ammonium Hydroxide (NH_4OH, 28.0-30.0%), Ethylene glycol (EG, 99.8%), Formaldehyde (36.5-38%), TRITON X-100, were purchased from Sigma-Aldrich (St. Louis, MO, USA). Cyclohexane was purchased from J.T.Baker. All reagents were used without further purification.

Synthesis of Silica Nanoparticles (SiO_2NPs)

Stöber method

The synthesis with Stöber method was conducted following the procedure described in Stöber *et al.* with some modifications (Stöber 1968). Briefly, ethanol (5 mL), and TEOS (100 µL) were stirred with milliQ water (20 mL) and NH_4OH solution (28.0-30.0%, 10 mL) for 2 hours at room temperature. Then, the reaction was blocked with acetone and centrifuged at 4000 rpm for 20 minutes. The silica nanoparticles were rinsed with milliQ water and acetone (1:1) 5 times.

Microemulsion Method

The quaternary W/O microemulsion was prepared at room temperature by mixing water, an organic solvent (Cyclohexane), a surfactant (Triton X-100) following the methods of Malvindi *et al*. (Malvindi 2012) Briefly, 880 µL of Triton X-100 was mixed with 3.75 mL of cyclohexane and 900 µL of 1-butanol for 30 minutes. Then, 170 mL of water, 50 µL of TEOS and 30 µL of NH_4OH were added to the microemulsion. After 24 h, the suspension was separated by centrifugation (4500 rpm) followed by 5 washes in ethanol and milliQ water. The nanoparticles were then redispersed in water.

Synthesis of SiO_2@Ag core/shell nanoparticles

250 mg of SiO_2NPs were dialyzed against pure water for 2 h in dialysis membrane tube (dialysis tubing cellulose membrane, Ø76 mm, NMWL 12,400 Sigma-Aldrich). The sample was purified 3 times with a high amount of ethanol. Sn^{2+} functionalized NPs were obtained by mixing them with 40 mL of $SnCl_2$ 0,070 M, under vigorous stirring (1500 rpm) for 1 h. After three steps of centrifugation, the SiO_2NPs were transferred to a 10 ml solution of ammoniacal silver nitrate $AgNO_3$ (0,40 M), excess of 3 mM of PVP (Mw~55,000), dissolved in ethylene glycole and formaldehyde/NH_4OH (1:1 ratio) at room temperature in order to obtain silver shell. Pure NPs were obtained by membrane filtration, three washes with ethanol followed by centrifugation steps (10000 rpm).

Nanoparticles characterizations (TEM, SEM, EDS, DLS, ζ-Potential, UV-Vis,)

Transmission electron microscope (TEM) characterizations were carried out with a JEOL Jem 1011 microscope, operating at an accelerating voltage of 100 Kv (JEOL USA, Inc). TEM samples were prepared by dropping a dilute solution of NPs in water on carbon-coated copper grids (Formvar/Carbon 300 Mesh Cu). Scanning Electron Microscopy (SEM) Energy-Dispersive X-ray Spectroscopy (EDS) were recorded with a Phenom ProX microscope (Phenom-World B. V., Eindhoven, Germany), at an accelerating voltage of 10 kV. The samples were prepared by dropping a solution of NPs in water on monocrystalline silicon wafer.Dynamic Light Scattering (DLS) and ζ-potential measurements were performed on a Zetasizer Nano-ZS equipped with a 4.0 mW HeNe laser operating at 633 nm and an avalanche photodiode detector (Model ZEN3600, Malvern Instruments Ltd., Malvern, UK). Measurements were made at 25°C in aqueous solutions (pH 7).The optical absorbance spectra of SiO_2NPs@Ag were measured with a Cary 300 UV–vis spectrophotometer (Varian,Palo Alto,USA) at a resolution of 1 nm using a 5 mm path length quartz cuvettes.

Cell culture

HeLa cells were maintained in high glucose DMEM with 50 µM glutamine, supplemented with 10% FBS, 100 U/mL penicillin and 100 mg/mL streptomycin. Cells were incubated in a humidified controlled atmosphere with a 95% to 5% ratio of air/CO_2, at 37°C.

Uptake of SiO_2@Ag NPs

To estimate the intracellular nanoparticles uptake, 10^5 cells were seeded in 1 mL of medium in each well of a 6-well plate. After 24 h of incubation at 37 ºC, the medium was replaced with fresh medium containing the nanoparticles at concentrations of 0.05 nM, 0.2 nM and 0.5 nM. After 48 and 96 h of incubation at 37 ºC, the medium was removed; the cells were washed three times with PBS (pH 7.4), trypsinized, and counted using a cell-counting chamber. Then, the cell suspensions were digested using 1 mL of concentrated HNO_3 10% (v/v) and the intracellular silver concentration was measured by means of elemental analysis and normalized to the number of cells.

WST-8 Assay

HeLa cells were seeded in 96 well microplates at concentration of 5.000 cells/well after a 24h of stabilization of the cells. Nanoparticles suspension stock solution was added to the cell media in order to obtain final concentrations of 0.05 nM, 0.2 nM and 0.5 nM for 48h and 96h. At the end of exposure, vitality was determined using a standard WST-8 assay (Sigma). Assays were performed following the procedure previously described in Malvindi *et al. (*Malvindi 2012). Data were expressed as mean ±SD. Differences in cell proliferation (WST-8) between cells treated SiO_2NPs@Ag and the control were considered statistically significant performing a *t*-student test with a p-value < 0.05.

Lactate dehydrogenase (LDH) leakage assay

Cells were treated with SiO_2@Ag NPs following the procedures reported for the WST-8 assay. The lactate dehydrogenase (LDH) leakage assay was performed on microplates by applying the CytoTox-ONE Homogeneous Membrane Integrity Assay reagent (Promega). The culture medium was collected and the level of lactate dehydrogenase (LDH) was measured by reading absorbance at 490 nm using a Bio-Rad microplate spectrophotometer. Data were expressed as mean ± SD.

Differences in LDH leakage between cells treated with NPs and controls were considered statistically significant performing a t-student test with SiO_2@Ag NPs a p-value < 0.05.

2′,7′-Dichlorofluorescein diacetate (DCF-DA) assay

HeLa cells were seeded in 96-well microplates and treated with NPs at a final concentration of 0.05, 0.2 and 0.5 nM. After 48 and 96 h of cell–NP interaction the DCF-DA (2′,7′-dichlorofluorescein diacetate, Sigma) assay was performed onto microplates following the procedure reported by De Matteis *et al.* (De Matteis 2016). Data were expressed as mean ± SD. Differences in ROS generation between cells treated with SiO_2NPs@Ag and controls were considered statistically significant performing a student *t* test with a P-value < 0.05.

Comet assay

HeLa cells were exposed to 0.5 nM of NPs for 48 h at density of 5×10^4 in each well of 12-well plates in a volume of 1.5 mL. After treatments, cells were centrifuged and suspended in 10 µl of PBS at concentration of 1000 cells/µl. The cell pellets were mixed with 75 µl of 0.75% low-melting-point agarose (LMA) and then layered onto microscope slides precoated with 1% normal melting agarose (NMA) and dried at room temperature. Subsequently, the slides were immersed in an alkaline solution (300 mM NaOH, 1 mM Na_2EDTA, pH 13) for 20 min to allow for unwinding of the DNA. The electrophoresis was carried out in the same buffer for 25 min at 25 V and 300 mA (0.73 V/cm). After electrophoresis, cellular DNA was neutralized by successive incubations in a neutralized solution (0.4 M Tris–HCl, pH 7.5) for 5 min at room temperature. The slides were stained with 80 µl SYBR Green I (Invitrogen). Comets derived from single cells were photographed under a Nikon Eclipse Ti fluorescence microscope (Nikon Instruments Europe B.V), and head intensity and tail length of each comets were quantified using Comet IV program (Perceptive Instruments).

Measurements of NP_S ions release

Silver ions release was quantified in three different conditions: by incubating SiO_2@AgNPs at pH 6.5 and 37 °C (acidic medium with ultrapure water and HCl to obtain pH 6.5), in neutral conditions (ultrapure water, pH 7) at 37 °C, and physiological condition (DMEM, pH 7.4) at 37 °C. The release was studied upon 24 h, 48 h, 72 h and 96 h of incubation time. The nanoparticle suspensions were diluted in the different solutions at a final concentration of 10 nM. After 24, 48, 72 and 96 h, the NPs were collected by centrifugation at 13000 rpm for 1 hour and digested by the addition of a solution of HNO_3 10% (v/v). The amount of free ions was measured by ICP-AES (Inductively Coupled Plasma Atomic Emission Spectrometer, Varian Inc.-Palo alto, USA).

All the instruments used to carry out the above mentioned experimental activities belong to Università del Salento - Dipartimento di Matematica e Fisica E.De Giorgi, Dipartimento di Ingegneria dell'Innovazione (Lecce, Italy) and to Department of Chemistry, University College London (London,UK).

Results

Core/shell nanoparticles represented an interesting class of nanomaterials indeed, as they can combine the physicochemical properties of two distinct materials, thus creating a nano-object with new properties. However, an important – and quite always neglected – aspect was the synthesis of highly controlled nanoparticles, especially for biological applications.

Synthesis of SiO_2NPs spheres. The synthetic route to obtain highly monodisperse SiO_2NPs@Ag were optimezd. In particular, we observed that a preliminary population of SiO_2NPs seeds was mandatory to uniformly deposit a silver shell around them. For this reason, two different procedures for the synthesis of SiO_2NPs were tested and compared, with the final aim to obtain the best possible preliminary sample of NPs seeds: the Stöber (Fig.1 A-B) and microemulsion method (Fig.1 C-D).

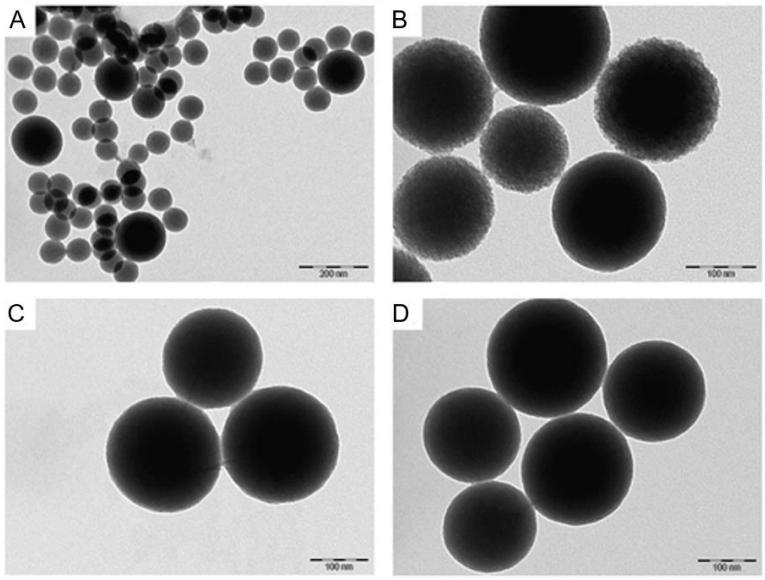

Figure 1. Representative TEM images of SiO_2NPs synthetized by the Stöber method (A-B) and microemulsion method (C-D).

Whilst the Stöber led to a quite polydisperse population of NPs (polydispersion index around 0.9%), also in terms of surface charge (Table 1), the microemulsion enabled the production of highly monodispersed samples with a size of about 180 nm (PDI of c.a. 0,15%). Moreover, the TEM characterizations of Figure 1 (C-D) clearly show that the formation of NPs having a smooth and uniform surface were induced by microemulsion method. In addition, a complete characterization of SiO_2NPs in figure 2 was shown. By UV-vis spectra measurements of SiO_2NPs nobody peak was displayed (Figure 2C).

Silica Nanoparticles (SiO_2NPs)	**Dynamic Light Scattering (DLS) ± standard deviation (SD)**	**Polidispersity Index (PI)**	**ζ –Potential ± standard deviation (SD)**
Stöber	190 ± 19 nm	0,9 %	-45 ± 3 mV
Microemulsion	180 ± 2 nm	0,15 %	-53 ± 2 mV

Table 1. Physicochemical characterizations of SiO_2NPs synthetized with either the Stöber (up row) and microemulsion (bottom row) methods.

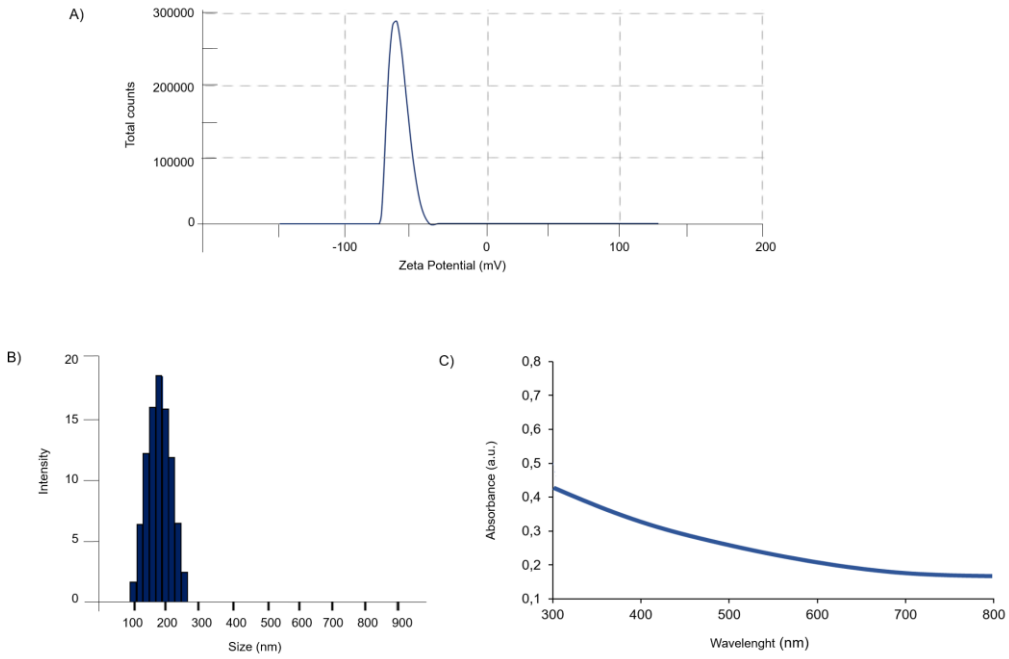

Figure 2. Characterization of SiO_2NPs obtained with microemulsion method. (A) ζ-potential measurements. (B) DLS characterization and (C) UV-Vis spectrum.

Synthesis of SiO_2NPs@Ag. The microemulsion method (see experimental section for more details) we then used to further functionalize the NPs surface with $SnCl_2$, in order to have a Sn^{2+} modified surface. This functionalization was a critical step, because the Ag^+ reduction was promoted by Sn^{2+}. A thorough and uniform Sn^{2+} surface coating was confirmed by the ζ-potential analyses of Figure 1S, as the surface charge value switched from -54 mV (before functionalization) to 45 mV (after the reaction with $SnCl_2$). We found this step crucial for promoting the formation of a uniform silver film around the silica seeds. The concentration of both SiO_2NPs and $AgNO_3$ ammonical silver nitrate were then optimized, in presence (or not), of PVP as colloidal stabilizer. As shown in Fig. 2AS, the use of $AgNO_3$ 0.20 mol/L^{-1} $AgNO_3$, without PVP, together with a constant NH_4OH: formaldeyde molar ratio (1:1) did not lead to uniform coatings after 10 minutes of reaction time. At a first glance, SiO_2NPs resulted almost uncoated, and only few random Ag nanoclusters were observed on the NPs surface. We speculated that the limitation could be ascribed to the low concentration of $AgNO_3$ (20 mol/L^{-1}). In a further attempt, the concentration of ammonical $AgNO_3$ (0.40 mol/L^{-1}) was increased. In this case, the formation of a silver shell around the silica surface was observed. However, uncontrolled

silver reduction also occurred (Fig. 2BS), which resulted in an inhomogeneous silver shell surrounding the SiO_2NPs surface. The synthetic rout with respect to previous approaches (Fig. 2CS) was improved, after addition of small volume of PVP, together with the use of $AgNO_3$ 0.20 mol/L^{-1}, despite we were still lacking NPs uniformity. While combining $AgNO_3$ 0.40 mol/L^{-1} with PVP (3 mM) The optimal synthetic conditions were achieved. In this case, the silver shell was demonstrated to perfectly surround the surface of silica seeds, and no silver aggregates were observed as well (Fig. 2).

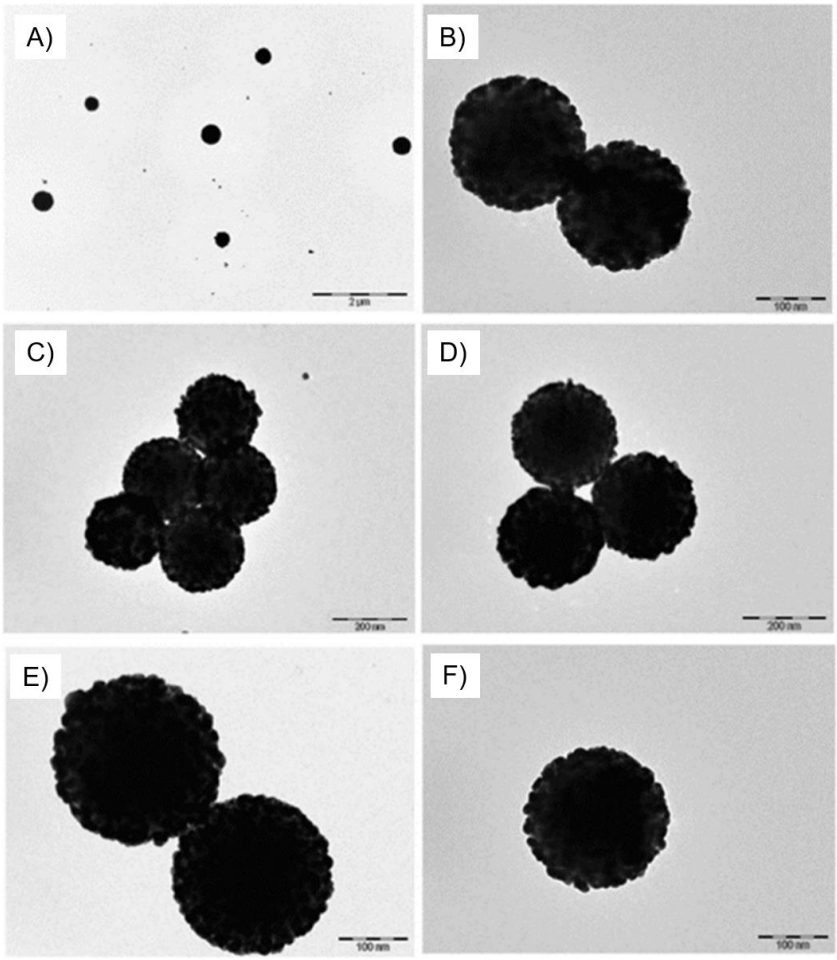

Figure 3. A-B-C-D-E-F) Representative TEM images of SiO_2NPs@Ag with PVP (3 mM), $AgNO_3$ (0.40 mol/L^{-1}) Formaldehyde:NH_4OH 1:1.

The growth of silver shell onto SiO_2 spheres were analyzed during the deposition of silver from 0 to 10 minutes by means of UV-vis measurements. Changes of shell thickness with time were observed; consequently, the absorption peak underwent a red shifting from the visible window. At ten minutes,

at a longer wavelength (around 500 nm) a new peak appeared which indicated the presence of 40 nm silver shell (Fig. 3SA). These data were supported by DLS measurements conducted on SiO2NPs: the deposition of silver started in the interval of reaction time from 2 minutes to 10 minutes. Size increase of the silver shell from 15 to 40 nm (3SB) was observed. A short summary of the synthesis procedure in Fig. 4S was schematized. ζ-potential analyses and DLS confirmed a surface charge of -16 mV and an average NPs diameter of about 220 nm and (Fig. 3A-3B), respectively. Indeed, UV-vis characterizations (Fig.4 C) and SEM-EDS analysis (Figure 5 A-B) further corroborated the presence of the silver shell on the SiO_2NPs.

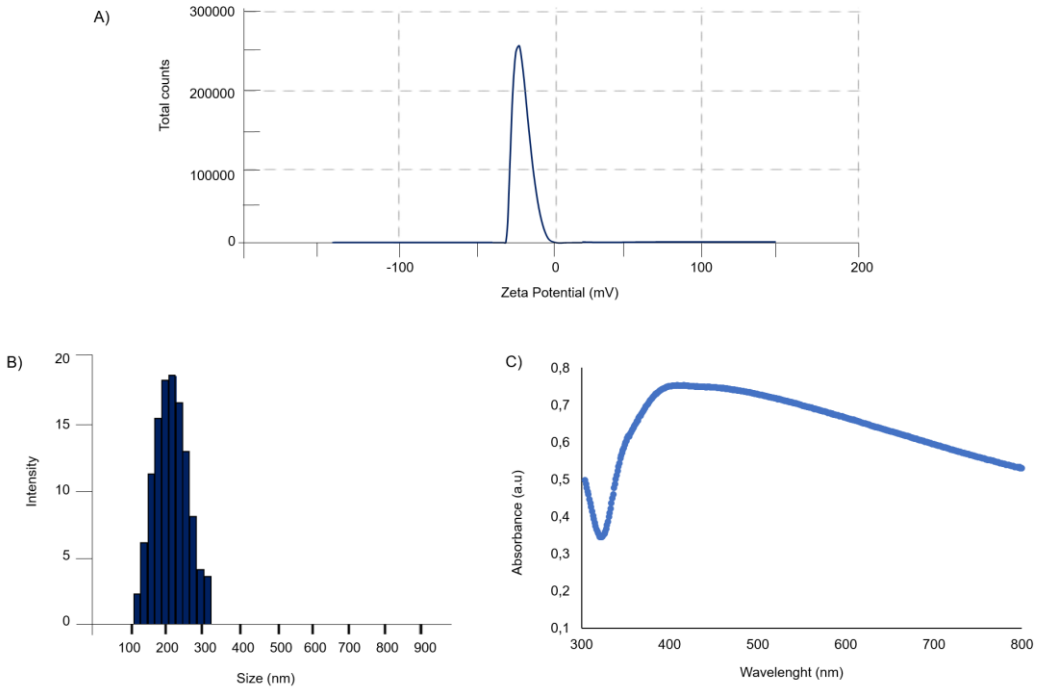

Figure 4 Characterization of SiO_2NPs@Ag shell synthetized via microemulsion method. **(A)** ζ-potential measurements. **(B)** DLS characterization and **(C)** UV-Vis spectrum.

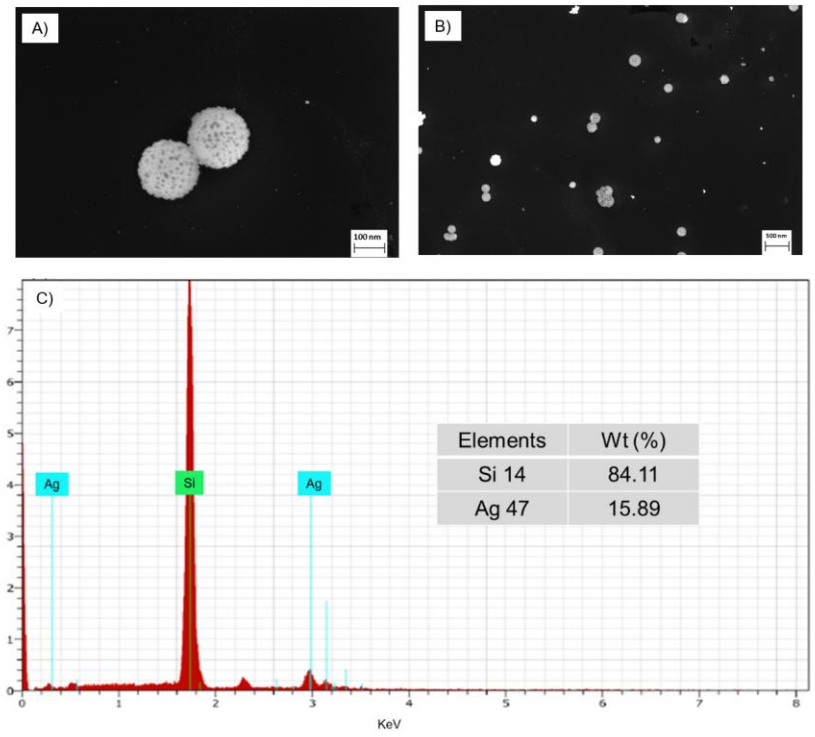

Figure 5. A-B) Representative SEM images at different magnification of SiO_2@AgNPs. C) EDS measurement of SiO_2@AgNPs.

Stability of SiO_2@Ag NPs. In oder to evaluate the stability of synthetized NPs, before making *in vitro* experiments, in water and DMEM up to 96h were analyzed. As shown in figure 6A) the DLS analysis demonstrated an increase of NPs size due to protein corona formation in DMEM (around 240nm at 96h) whereas in water this effect was negligible. Furthermore, the evaluation of broader red-shifted absorption peak in the UV–vis suggested the presence of some aggregations at 72 h and 96 h. The stability of AgNPs coated with PVP for a long period (21 days) was analyzed by previous works (Sharma 2014, Tejamaya 2012) showing a good stability data. Also in our case, the stability up to 21 days was similar to the results obtained at 96 h. Figure (S5).

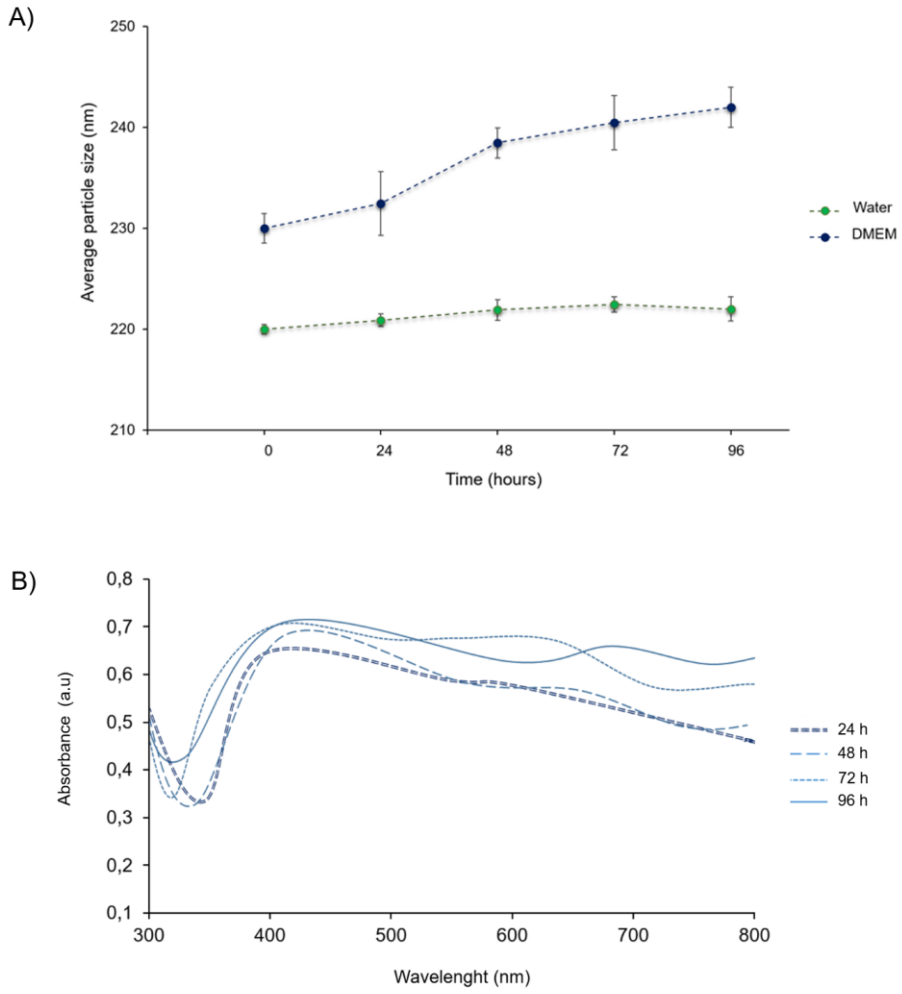

Figure 6 Stability of SiO_2@Ag NPs ,A) average DLS measurements performed at 0, 24, 48, 72, 96h in water and in DMEM. B) Uv-vis spectra of NPs dispersed in DMEM after 24, 48,72,96h.

To complete the stability studies, DLS and zeta potential measurements of SiO_2@AgNPs suspended In DMEM in order to obtain a final concentrations of 0.05 nM ,0.2 nM,0.5 nM, (that were the same used for further toxicology assays) were performed (Table 2)

SiO_2@AgNPs	**Dynamic Light Scattering (DLS) ± standard deviation (SD)**	**ζ –Potential ± standard deviation (SD)**
0.05 nM	240 ± 3	-25 ± 6 mV
0.2 nM	241 ± 2	-25 ± 2 mV
0.5 nM	240 ± 5	-27 ± 3 mV

Table 2. Characterization of SiO_2@Ag NPs at three concentrations in DMEM.

After optimising the fabrication procedures, we moved on testing *in vitro* the effects of these SiO_2@Ag NPs using HeLa cell lines as a model system.

Internalization of SiO_2@Ag NPs by HeLa cells. As a preliminary investigation, the quantification of the uptake levels of SiO_2@Ag NPs was analyzed. We thus carried out inductively coupled plasma atomic emission spectroscopy (ICP-AES) elemental analysis over cell lysate, after incubating HeLa cells with the three concentrations (0.05 nM, 0.2 nM and 0.5 nM) of NPs. The time-dependent internalization of NPs in HeLa cells was confirmed by experimental data. In particular, cells underwent an uptake of c.a. 0.2 picomolar of NPs after 48 hours, and this raised up to c.a. 0.4 picomolar after 96 hours of incubation time with the higher concentration tested (Fig. 7A). Representative optical microscopy acquisition of NPs uptake in HeLa cells, after 48 and 96 hours, were displayed in Fig. 7B.

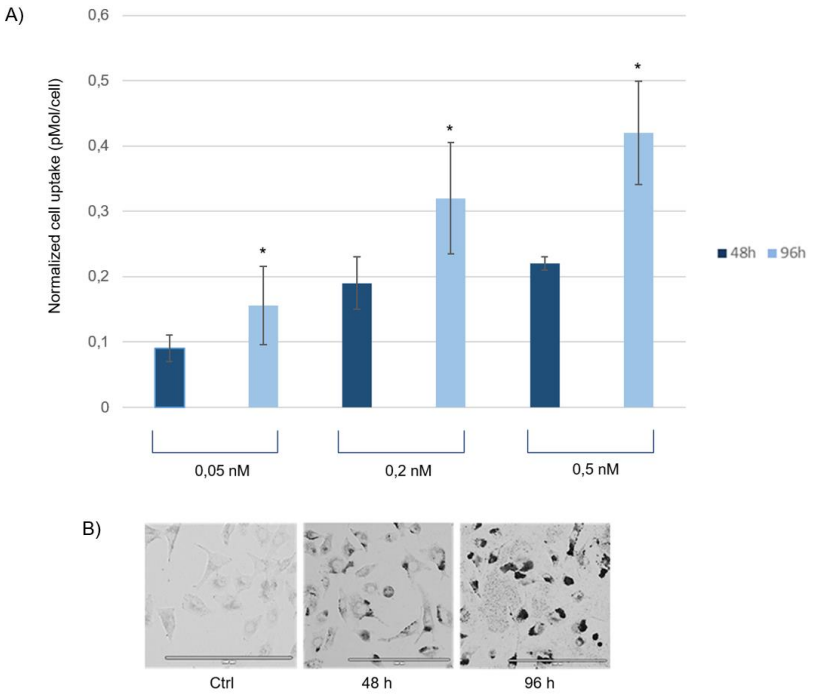

Figure 7. A) Normalized internalization data for HeLa cells expressed as picomolar of SiO_2@Ag NPs nanoparticles internalized (determined by ICP-AES) per cell after 48 and 96 h of NPs incubation at three concentrations (0.05, 0.2 and 0.5). Data are reported as mean ± SD from three independent experiments. B) Optical microscope images acquired after 48 and 96h of SiO_2@AgNPs at concentration of 0.5nM.

Cellular toxicity assays. The viability (WST-8 assay), the membrane integrity (LDH assay), the ROS levels production (DCFH-DA assay), and the DNA damage (Comet assay) upon NPs incubation were characterized. three NPs concentrations (0.05, 0.2, 0.5 nM), for different incubation times (24 h, 48 h, 72 h, 96 h) were tested. The selection of the 0.05 nM, 0.2 nM, 0.5 nM concentrations of SiO_2@Ag NP was based on a preliminary study undertaken to assess the response to different dose (data not shown). Negligible cytotoxicity in HeLa cells with concentration lower than 0.05 nM was showed, whereas a precipitation in DMEM after 96h at concentration higher than 0.5 nM was induced. SiO_2@Ag NPs were found to reduce cell viability in a dose dependent manner: a 30 % decrease in viability after 96 h of incubation time at the higher concentration tested (Fig. 8A) were observed. The analysis of LDH release indicates that NPs induce cell membrane damage (Fig. 8B), in close agreement with the viability results. Moreover, the potential NPs-induced oxidative stress, by DCFH-DA assay was evaluated. The interaction between NPs and cells stimulated the generation of Reactive Oxygen Species (ROS), again in a dose dependent manner (Figure 8C).

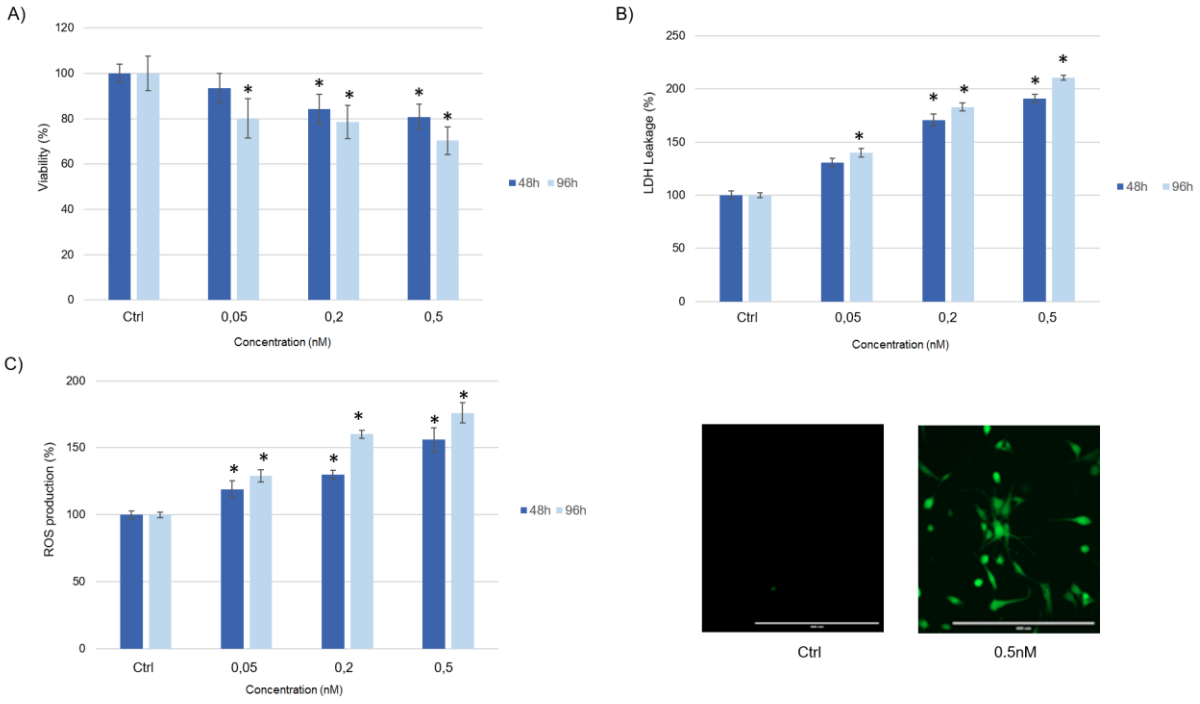

Figure 8. **A)** Normalized viability assay (WST-8) of Hela cells after 48 h and 96 h exposure to 0.05, 0.2, 0.5 nM of SiO_2@Ag NPs. As positive control (P), cells were incubated with 5% DMSO (data not shown). Data are reported as mean ± SD from three independent experiments; *P < 0.05 compared with control (n= 8). **B)** LDH assay on HeLa cells incubated with increasing concentrations of SiO_2@Ag NPs (0.05 nM,0.2 nM and 0.5 nM) at different times (48 and 96 h). Percent of LDH leakage of nanoparticle-treated cells are expressed relative

to non-treated control cells. Positive controls (P) consisted in the treatment of cells with 0.9% Triton X-100 showing ca. 500 % LDH increase (data not shown). Data are reported as mean ± SD from three independent experiments; *P < 0.05 compared with control (n= 8). **C)** Left: Effect of SiO_2@Ag NPs on the ROS level in HeLa cells. Cells were treated with nanoparticle concentrations (0.05, 0.2, 0.5 nM) for 48 h, incubated with 100 µM DCFH-DA and the cells fluorescence was measured. As a positive control (P), cells were incubated with 500 µM H_2O_2 showing a ca. 300% DCFH-DA increase (not shown). Data are reported as mean ±SD from three independent experiments; *P<0.05 compared with control (n= 8). Right: Representative fluorescence images of HeLa cells treated for 48 h with 0.5 nM SiO_2@Ag NPs and incubated with DCFH-DA (100 µM).

Finally the effects of NPs on DNA were tested, using the comet assay. The formation of long comet tails on cells induced by SiO_2@AgNPs were observed, which indicated a remarkable damage to DNA (Fig. 9). Similarly, also the comet head (i.e., the cell nucleus) changed morphology and dimension upon NPs treatment, indicating events of DNA stress.

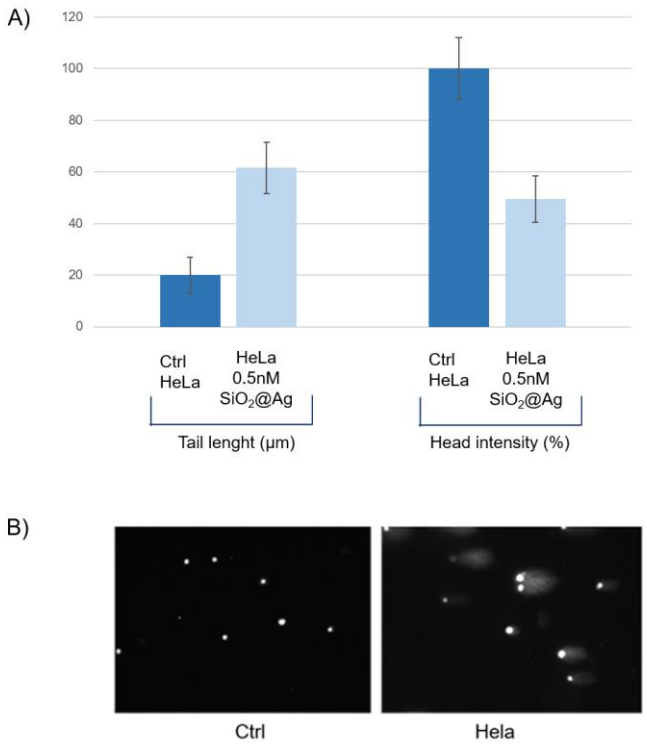

Figure 9. Comet assay experiments to verify the DNA damage of HeLa cells due to SiO_2@Ag NPs. HeLa cells were treated with 0.5 nM of NPs for 48 h. A) DNA damage was evaluated by tail length (µm) and head intensity (%). Values represented the average of 100 randomly selected comet images of each sample. As a positive control (P) cells were incubated with 500 µM H_2O_2 (data not shown). B) Representative images of SiO_2@Ag NPs effect on DNA damage in HeLa cell lines. Data are reported as mean ±SD from three independent experiments; *P < 0.05 compared with control (n= 3)

Degradation of SiO_2@AgNPs. After the cytotoxicity and genotoxicity assays, nanoparticles degradation phenomena were investigated. We hypothesized that the toxicity of SiO_2@Ag core/shell nanoparticles might be ascribed to the silver ions release promoted by the low pH, in the (acidic) tumor microenvironment. To confirm this hypothesis the ions released from SiO_2@Ag NPs at 37°C in acidic conditions (acidic medium with ultrapure water and HCl, pH 6.5), and in neutral and physiological conditions (ultrapure water and DMEM, pH 7 and 7.4 respectively) were analysed. The NPs dissolution in the two conditions was measured again by ICP elemental analysis. A direct dependence between silver ionization and acidic environment (Fig. 10) was demonstrated. In particular, an increase of silver ions release from 0.05 µM after 24 hours to 0.16 µM after 96 hours, at a pH value of 6.5 were observed. These data were corroborated with the lack of silver release under neutral and physiological pH (both in water and in the DMEM cell culture media).

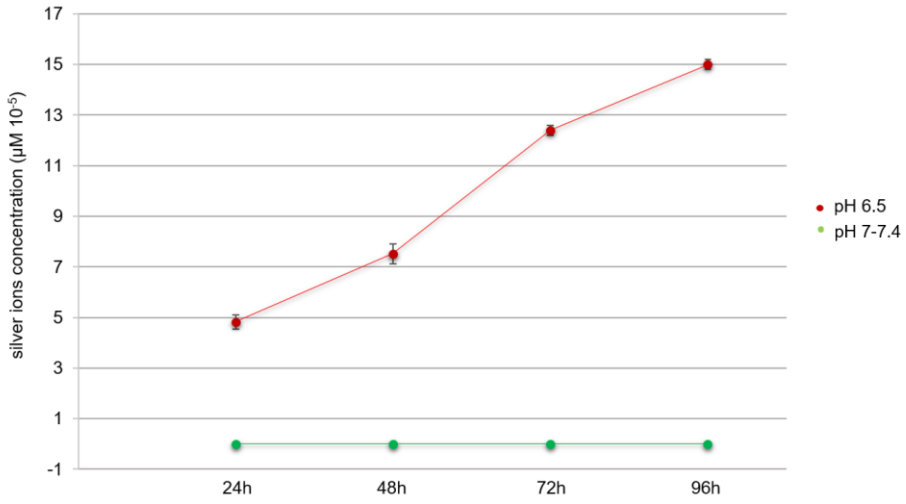

Figure 10. Effects of time and pH on silver ions release from SiO_2NPs@AgNPs degradation was evaluated at pH 6.5 , 7 (ultrapure water) and 7.4 (DMEM) up to 96 h.

DISCUSSION

The design of new and unforeseen classes of materials, especially for biomedical application, constantly challenges material scientists. (Tibbitta 2015). The revolution of nanotechnology, established some decades ago, is nowadays routinely used as a tool for exploring and characterising new materials (Koo 2005). However, a big issue is always represented by the difficulty in finely tuning the material physicochemical properties at the nanoscale, in order to create nano-objects with unique and reproducible characteristics (Fenwick 2016). Silver represented a potential anticancer nanomaterial through your toxicity properties. For example, in a recent work (Zhan 2017), the anticancer activity of camptothecin (anti-cancer agent) decorated by AgNPs in MCF7 and MDAMB231 were investigated. The authors showed strong cytotoxicity against cancer cells. In our work, we explored the toxicity profile of SiO_2@Ag core/shell nanoparticles, in the viewpoint of potential applications in drug discovery for cancer treatment. First, we carefully optimized the synthetic procedures for achieving highly homogeneous NPs. We found that the driving force in obtaining a uniform and smooth silver surface, covering the SiO_2 seeds, is the correct ratio between $AgNO_3$ and PVP (Fig. 2) with a pre-functionalization of $SnCl_2$, critical for optimizing the silver deposition. In general, the particles of a dielectric core as silica coated with a metallic shell as silver manifested a strong optical resonance dependent on shell thickness. (Zhou 2016) Having NPs with highly controlled physicochemical properties is mandatory in biomedical application, as NPs size, shape, and surface characteristics can differently impact cells behavior. In addition, another important aspect concerning the new synthetized SiO_2@$AgNP_S$ was the stability in cell culture media. This point is important for toxicological investigations. In particular, the protein corona induces an increase of NPs size and, at 72 h and 96 h, some aggregation phenomena. In this experimental work, this problem was solved using small concentrations of NPs. We then characterized the uptake rate of the SiO_2@Ag in time, finding a constant increase in the engulfed NPs up to 96 hours of incubation time. These data correlated well with the cytotoxicity studies. The preliminary viability assays confirmed, in fact, that NPs induced a concentration-dependent decrease in HeLa viability, which drops down also as a function of the incubation time, because of the higher up-taken material. The evidence of increased cell death led us to investigate the NPs toxicity mechanisms. The

membrane damage assay, based on the detection of the extracellular activity of the cytoplasmatic enzyme LDH, confirmed that NPs induce an extensive membrane damage (Fig. 8B). In order to understand whether this is a direct or indirect damage, we investigated the presence of intracellular reactive oxygen species (ROS). SiO_2@Ag core/shell NPs induce a significant increase in the presence of ROS, which can explain the high membrane damage (Figure 5C). However, it is also well established that intracellular ROS can harm the cellular genetic material, and for this reason, we carried out a comet assay. In this method, cells are lysed and the nuclei are loaded onto an agarose gel for electrophoresis. Any physical damage to DNA is then visualised as a comet tail, protruding from the 'head' represented by the nuclei. Our results confirm that SiO_2@Ag NPs can damage the DNA, a process leading to the formation of long comets. Taken together, the data demonstrate that the damage induced by NPs is not due to a physical interaction with cellular and sub-cellular components, but rather due to the generation of ROS, which, in turns, are at the base of the observed cyto - and genotoxicity. There is always the big opening question whether the detected effects are induced by the NPs themselves, or by the silver ions releasing from their surfaces. Previosuly work have demonstrated that strong acidic environment, characterising the early endocytic vesicles of cells and lysosome, strongly promotes Ag+ release in time (Reidy 2013, Wildt 2015) representing a good opportunity for the development of new drug delivery systems for cancer treatment as well. Therefore, the extracellular environment of tumor cells is important in order to design nano-objects responsive to pH. Indeed the pH is reduced in tumor tissue compared to normal ones where it is relatively basic (Gerweck, 1996). For this reason we investigated this phenomenon in a media that mimicks tumor microenvironment that has typical acidic characteristics (pH 6.5), which can promote silver ions release, thus triggering a local and controlled cytotoxicity. In neutral and physiological conditions (water and DMEM) any ionization phenomenon did not occur, suggesting the appropriate use of our nano-object in tumor conditions. Indeed the "onion" structure typical of core/shell nanoparticles stabilized with PVP could represent a dual advantage compared to AgNPs coated with PVP in cancer treatment. First, the metallic shell thickness can be customized in order to have a different amount of metal around to silica core and then a different amount of ions released. Furthermore, the degradation phenomena which occur in the acidic microenvironment

surrounding cells in the pathological state, can induce toxicity before the endocytosis process, and consequently an increase of the general toxic effects induced by the subsequent uptake. An antitumoral drug internalized in the silica core can be released after silver shell ionization. As they represent a dual mechanism of action, our monodisperse and stable SiO_2@AgNPs could represent a powerful drug carrier for cancer treatment. Further studies will projected to study the silver ions release from SiO_2@AgNPs directly in tumoral tissues.

CONCLUSIONS

The field of nanomedicine is constantly evolving, giving birth to new generations of nanomaterials with several biomedical applications. In this work, we investigated the interactions between SiO_2@Ag core/shell NPs and HeLa cells. In, particular, after optimizing the best chemical routes for synthetizing highly controlled NPs (in terms of narrow size and shape distribution), we firstly explored NPs effects on cells viability. We correlate the decrease in HeLa viability with the increase in uptake levels during time. We found that the main cause of toxicity to cells is the formation of intracellular ROS, which damage both the cell membrane (releasing the LDH enzyme) and the DNA at the same time. We found that ROS generation is caused by the presense of silver ions, released from the NPs surface upon interaction with acidic environment typical of tumor extracellular space unlike neutral and physiological conditions. We believe this nanomaterial can represent a good opportunity for the next development of drug delivery system. Our core/shell NPs can combine, in fact, a good intracellular and intra-tissue tracking (e.g. through functionalization of the silica core with fluorescent reporters) or capsules to confine antitumoral drugs, together with a local and controlled induction of toxicity.

AUTHOR INFORMATION

Corresponding Author

*E-mail: valeria.dematteis@unisalento.it

Conflict of interest

The authors declare that they have no conflict of interest.

References

Amendola V, Bakr OM, Stellacci F (2010) A Study of the Surface Plasmon Resonance of Silver Nanoparticles by the Discrete Dipole Approximation Method: Effect of Shape, Size, Structure, and Assembly, Plasmonics, 2010, 5, 85–97.

Banerjeea A, Qia J, Gogoic R, Wonga J, Mitragotri S (2016) Role of nanoparticle size, shape and surface chemistry in oral drug delivery. J of Controlled Rel. 238, 28, 176–185.

Cassagneau T, Caruso F (2002) Contiguous Silver Nanoparticle Coatings on Dielectric Spheres, Adv. Mater, 14, 732.

Chang TH, Chang YC, Ko FH, Liu FK (2013) Electroless Plating Growth Au-Ag Core-Shell Nanoparticles for Surface Enhanced Raman Scattering, Int J Electrochem Sci, 8, 6889 – 6899.

Chen G, Roy I, Yang C, Prasad PN (2016) Nanochemistry and Nanomedicine for Nanoparticle-based Diagnostics and Therapy. Chem. Rev., 116 (5), 2826–2885.

Choma J, Dziuran A, Jamioła D, Nyga P, Jaroniec M (2011) Preparation and properties of silica–gold core–shell particles, Colloids Surf. A , 373, 167−171.

De Matteis V, Cascione MF, Brunetti V, Toma CC, Rinaldi R (2016) Toxicity assessment of anatase and rutile titanium dioxide nanoparticles: The role of degradation in different pH conditions and light exposure, Toxicol In Vitro, 37:201-210. doi: 10.1016/j.tiv.2016.09.010.

Dokoutchaev A, James JT, Koene SC, Pathak S, Prakash GKS, Thompson ME (1999) Colloidal Metal Deposition onto Functionalized Polystyrene Microspheres, Chem. Mater, 11 (9), 2389–2399.

Dong A, Wang Y, Tang Y, Ren N, Yang W, Gao Z (2002) Fabrication of compact silver nanoshells on polystyrene spheres through electrostatic attraction, Chem. Commun., 350−351.

Elbaz NM, Ziko L, Siam R, Mamdouh Wael (2016), Core-Shell Silver/Polymeric Nanoparticles-Based Combinatorial Therapy against Breast Cancer *In-vitro,* Scientific Reports | 6:30729 | DOI: 10.1038/srep30729

Elshawy OE, Helmy EA, Rashed LA (2016) Preparation, Characterization and in Vitro Evaluation of the Antitumor Activity of the Biologically Synthesized Silver Nanoparticles, Advances in Nanoparticles, 5, 149-166.

Fen LB, Chen S, Kyo Y, Herpoldt KL,Terrill NJ, Dunlop IE, McPhail DS, Shaffer MS, Schwander S, Gow A, Zhang JJ, Chung KF, Tetley TD, Porter AE, Ryan MP (2013) The Stability of Silver Nanoparticles in a Model of Pulmonary Surfactant, Environ Sci Technol. 1; 47(19): 11232–11240.

Fenwick O, Coutiño-Gonzalez E, Grandjean D, Baekelant W, Richard F, Bonacchi S, De Vos D, Lievens P, Roeffaers M, Hofkens J, Samorì P (2016) Nature Materials 15, 1017–1022.

Ganta S, Devalapally H, Shahiwala A, Amiji M (2008) A review of stimuli-responsive nanocarriers for drug and gene delivery, Journal of Controlled Release 126 187–204.

Gerweck LE and Seetharaman K (1996), Cellular pH Gradient in Tumor versus Normal Tissue: Potential Exploitation for the Treatment of Cancer, Cancer Research, 56, 1194-1 198.

Guo D, Zhu L, Huang Z, b, Zhou H, Ge Y, Ma W, Wu J, Zhang X, Zhou X, Zhang Y, Zhao Y, Gu N (2013), Anti-leukemia activity of PVP-coated silver nanoparticles via generation of reactive oxygen species and release of silver ions. Biomaterials 34, 7884–7894

Gurunathan S. Lee KJ, Kalishwaralal K, Sheikpranbabu S, Vaidyanathan R, Eom SH (2009), Antiangiogenic properties of silver nanoparticles. Biomaterials 30, 6341–6350.

Huang H, Lai W, Cui M, Liang L, Lin Y, Fang Q, Liu Y, Xie L (2016) An Evaluation of Blood Compatibility of Silver Nanoparticles, Scientific Reports, 6,25518, doi:10.1038/srep25518.

Jackson J, Halas N (2001) Silver Nanoshells: Variations in Morphologies and Optical Properties, J. Phys Chem B, 105, 2743−2746.

Jiang Zj, Liu Cy (2003) Seed-Mediated Growth Technique for the Preparation of a Silver Nanoshell on a Silica Sphere, J Phys Chem B, 107, 12411−12415.

Kanchana S, Santhanalakshm J (2017) Evaluation of in vitro anticancer potentials of pvp stabilized silver, copper and nickel nanoparticles, international journal of chemical and pharmaceutical analysis, 4, No 1.

Koo OM, Rubinstein I, Onyuksel H (2005) Role of nanotechnology in targeted drug delivery and imaging: a concise review, Nanomedicine: Nanotechnology, Biology and Medicine, 1, 3, 2005, 193–212.

Liu T, Li D, Yang D, Jiang M (2011) An improved seed-mediated growth method to coat complete silver shells onto silica spheres for surface-enhanced Raman scattering, Colloids and Surfaces A, 387, 1–3, 17–22.

Malvindi MA, Brunetti V, Vecchio G, Galeone A, Cingolani R, Pompa PP, Nanoscale, 2012, 4, 486-495

Nel AE, Mädler L, Velegol D, Xia T, Hoek EMV, Somasundaran P, Klaessig F, Castranova V, Thompson M (2009) Understanding biophysicochemical interactions at the nano-bio interface. Nat. Mat., 8, 543 - 557.

Nguyena KC, Richardsa L, Massarsky A, Moonb TW, Tayabalia AF (2016) Toxicological evaluation of representative silver nanoparticles in macrophages and epithelial cells. Tox in vitro, 33, 163–173

Oldenburg S, Averitt R, Westcott S, Halas N (1998) Nanoengineering of Optical Resonances, Chem. Phys. Lett., 288, 243−247.

Pol VG, Srivastava D, Palchik O, Palchik V, Slifkin M, Weiss A, Gedanken (2002) A Sonochemical Deposition of Silver Nanoparticles on Silica Spheres, Langmuir, 18, 3352−3357.

Reidy B, Haase A, Luch A, Dawson KA, Lynch I (2013) Mechanisms of Silver Nanoparticle Release, Transformation and Toxicity: A Critical Review of Current Knowledge and Recommendations for Future Studies and Applications Materials 6, 2295-2350.

Rieffel J, Chitgupi U, Lovell JF (2015) Recent Advances in Higher-Order, Multimodal, Biomedical Imaging Agents Small, 16;11(35):4445-61.

Rodrigues RO, Bañobre-López M, Gallo J. et al. (2016) Haemocompatibility of iron oxide nanoparticles synthesized for theranostic applications: a high-sensitivity microfluidic tool. J. Nanopart. Res. 18: 194. doi: 10.1007/s11051-016-3498-7

Schueler PA, Ives JT, DeLaCroix F, Lacy WB, Becker PA, Li J, Caldwell KD, Drake B, Harris JM (1993) Physical Structure, Optical Resonance, and Surface-Enhanced Raman Scattering of Silver-Island Films on Suspended Polymer Latex Particles, Anal. Chem., 65, 3177−3186.

Sharma VK,. Siskova KM, Zboril R, Gardea-Torresdey JL, Organic-coated silver nanoparticles in biological and environmental conditions: Fate, stability and toxicityAdv in Colloid and Interface Sci 204 (2014) 15–34.

Stöber W, Fink A, Bohn E (1968) Controlled growth of monodisperse silica spheres in the micron size range, J. Colloid Interface Sci, 26, 62.

Kneipp K, Dasari RR, Wang Y (1994) Near-Infrared Surface-Enhanced Raman Scattering (NIR SERS) on Colloidal Silver and Gold, Appl. Spectrosc, 48, 951−955.

Wei S, Wang Q, Zhu J, Sun L, Line H, Guo Z, (2011) Multifunctional composite core–shell nanoparticles, Nanoscale, 3, 4474-4502 DOI: 10.1039/C1NR11000D

Wildt BE, Celedon A, Maurer EI,. Casey BJ, Nagy AM, Hussain SM, Goering PL (2015): Intracellular accumulation and dissolution of silver nanoparticles in L-929 fibroblast cells using live cell time-lapse microscopy, Nanotoxicology, DOI: 10.3109/17435390.2015.1113321

Krystek P,Giannakou C, Hendriks AJ, de Jong WH (2016) Exploring the effect of silver nanoparticle size and medium composition on uptake into pulmonary epithelial 16HBE14o-cells, J. Nanopart. Res 18: 182. doi:10.1007/s11051-016-3493-z

Tejamaya M, Romer I, Merrifield RC, Lead JR (2012) Stability of citrate PVP, PVP, and PEG coated silver nanoparticles in ecotoxicology media. Environ Sci Technol 46:7011–7

Tibbitta MW, Rodell CB, Burdickb JA, KS Anseth (2015) Progress in material design for biomedical applications, PNAS 112,47: 14444–14451

Van der Zande M, Undas AK, Kramer E, Monopoli MP, Peters RJ, Garry D, Antunes Fernandes EC, Hendriksen PJ, Marvin HJP, Peijnenburg AA HBouwmeester (2016) Different responses of Caco-2

and MCF-7 cells to silver nanoparticles are based on highly similar mechanisms of action, Nanotoxicology, 10: 1431-1441.

Westcott SL, Oldenburg SJ, Lee TR, Halas NJ (2000) Construction of Simple Gold Nanoparticle Aggregates with Controlled Plasmon-Plasmon Interactions, Langmuir, 16, 6921.

Yang JK, Kang H, Lee H, Jo A, Jeong S, Jeon SJ, Kim HI, Lee HY, Jeong DH, Kim JH, Lee YS (2014) Single-Step and Rapid Growth of Silver Nanoshells as SERS-Active Nanostructures for Label-Free Detection of Pesticides, ACS Appl. Mater. Interf. 6, 12541−12549.

Zolghadri S, A Saboury A, Golestani A, Divsalar A, Rezaei-Zarchi S, Moosavi-Movahedi AA (2009) Interaction between silver nanoparticle and bovine hemoglobin at different temperatures. Journal of Nanoparticle Research 11, 1751–1758.

Zhan H, Zhou X, Cao Y, Jagtiani T, Chang TL, JF Liang (2017) Anti-cancer activity of camptothecin nanocrystals decorated by silver nanoparticles, J. Mater. Chem. B, DOI: 10.1039/c7tb00134g.

Zhou N, Yuan M, Gao Y, Li D, Yang D (2016) Silver Nanoshell Plasmonically Controlled Emission of Semiconductor Quantum Dots in the Strong Coupling Regime, ACS Nano,10 (4),4154–4163

Zsigmondy R. (1927) Kolloidchemie I and II; Spamer: Leipzig.

Supplementary materials

One-step synthesis, toxicity assessment and degradation in tumoral pH environment of SiO_2@Ag core/shell nanoparticles

Valeria De Matteis*[1], Loris Rizzello[2], Maria Pia Di Bello[3], Rosaria Rinaldi[1]

1. Università del Salento, Dipartimento di Matematica e Fisica “Ennio De Giorgi”, Via Arnesano, 73100 Lecce, Italy
2. Department of Chemistry, University College London, London, WC1H 0AJ, UK
3. Università del Salento, Dipartimento di Ingegneria dell’Innovazione, Via Arnesano, 73100 Lecce, Italy

Corresponding Author: *e-mail: valeria.dematteis@unisalento.it

KEYWORDS: core/shell nanoparticles; one-step synthesis; cytotoxicity; genotoxicity; pH tumor environment; ionization

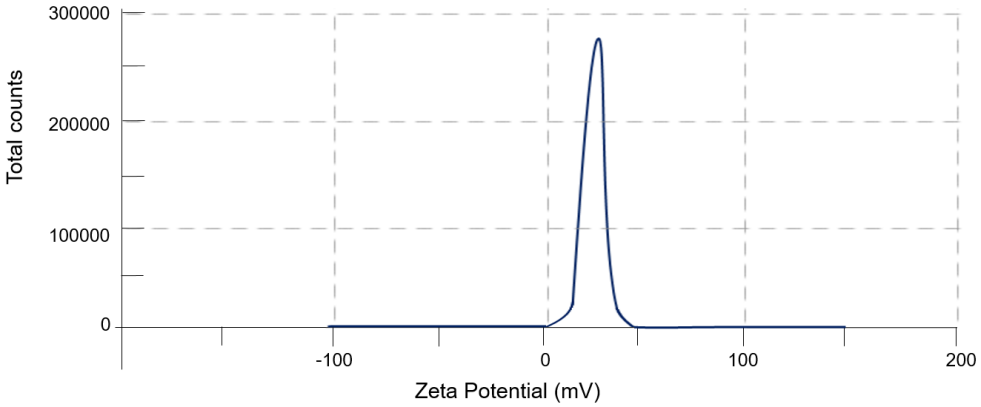

Figure 1. ζ -potential measurement of SiO_2NPs functionalized with $SnCl_2$

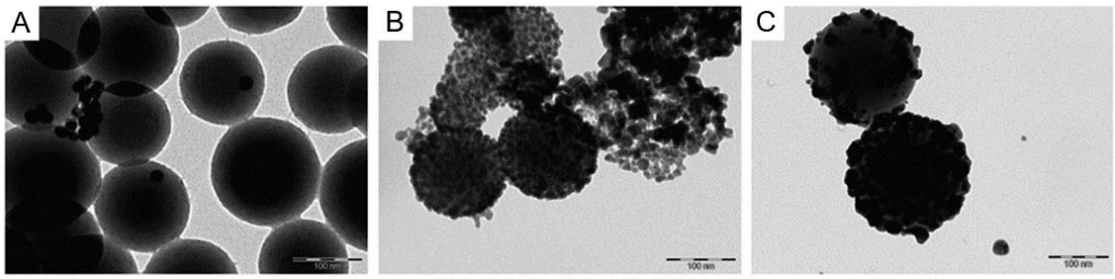

Figure 2. TEM images of **A)** SiO_2NPs@Ag without PVP, $AgNO_3$ [0,20 mol/L^{-1}] and Formaldehyde:NH_4OH 1:1, **B)** SiO_2NPs@Ag without PVP, $AgNO_3$ [0,40 mol/L^{-1}] Formaldehyde:NH_4OH 1:1, **C)** SiO_2NPs@Ag with PVP, $AgNO_3$ [0,20 mol/L^{-1}] Formaldehyde:NH_4OH 1:1. All synthesis are obtained keep constant the reaction time (10 minutes

A)

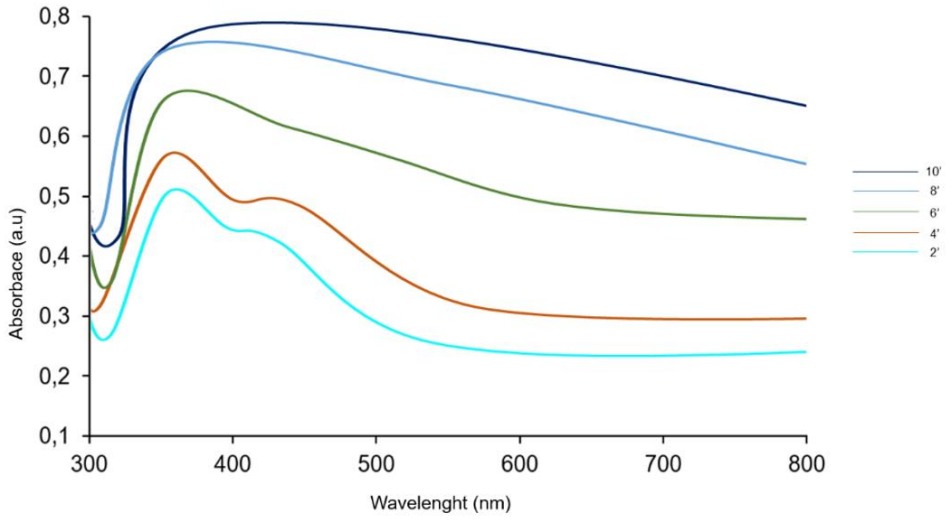

B)

Time (minutes)	silver shell size (DLS measurements ± SD)
2	5 nm ± 0.9
4	5.6 nm ± 1.5
6	10 nm ± 3
8	35 nm± 2.5
10	40 nm ± 2.8

Figure 3 A) Evolution of UV-vis spectra with the increasing of silver nanoshell thickness in time reaction time (10 minutes). B) thickness of growing silver shell in time acquired by DLS.

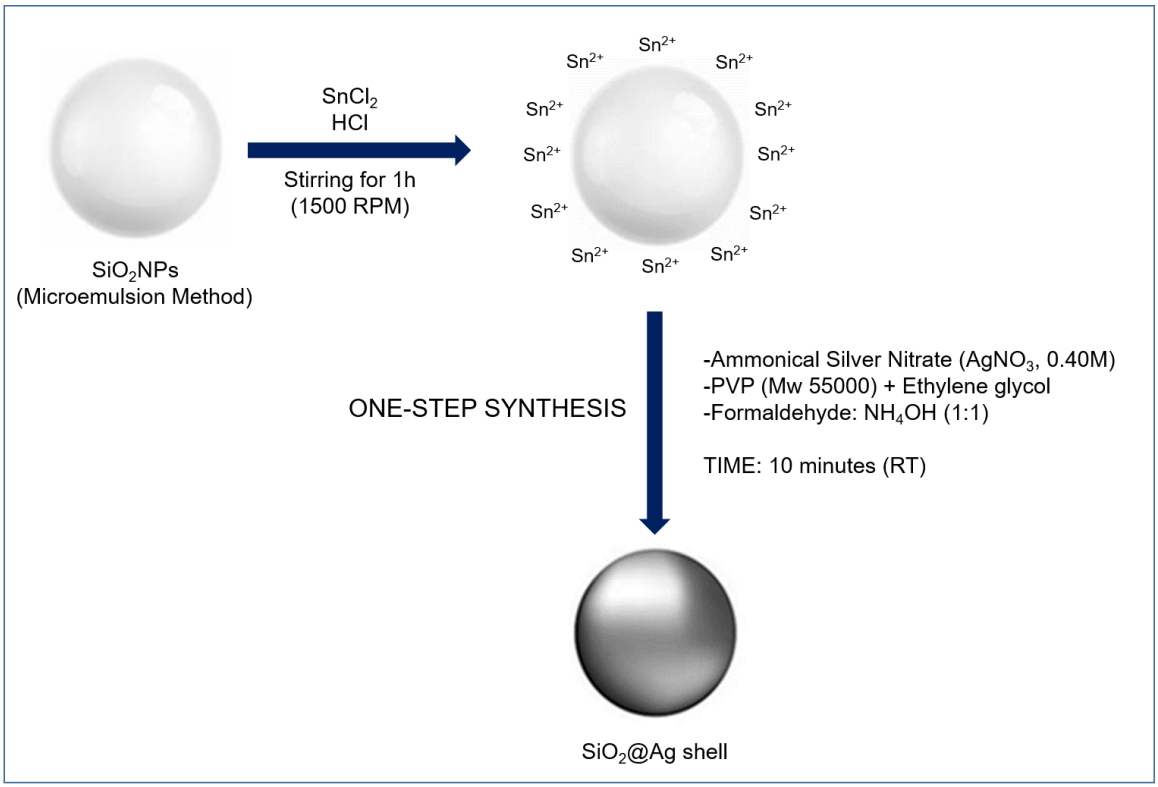

Figure 4. Schematic representation for the silver coating over the surface of the SiO_2NPs

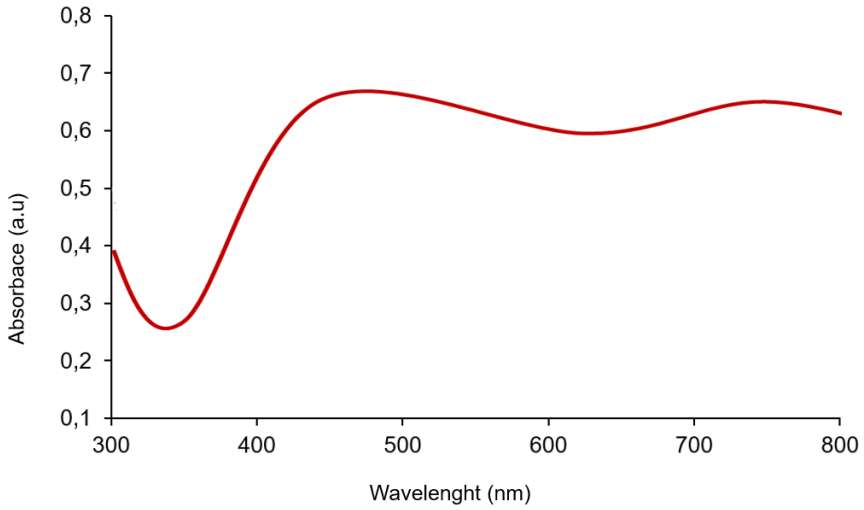

Figure 5. Uv-vis spectra of SiO_2@AgNPs dispersed in DMEM up to 21 days.